Grant agreement No. 640979

ShaleXenvironmenT

Maximizing the EU shale gas potential by minimizing its environmental footprint

H2020-LCE-2014-1
Competitive low-carbon energy

D9.1 – Application of well blowout model to an existing well to generate fire and explosion risk contours

WP 9 – Risk Assessment

Due date of deliverable	Month 18 – February 2018
Actual submission date	17 / 03/ 2017
Start date of project	September 1st 2015
Duration	36 months
Lead beneficiary	UCL
Last editor	Haroun Mahgerefteh
Contributors	Sergey Martynov (UCL), Haroun Mahgerefteh (UCL)
Dissemination level	Public (PU)

This Project has received funding from the European Union's Horizon 2020 research and innovation programme under grant agreement no. 640979.

Disclaimer

The content of this deliverable does not reflect the official opinion of the European Union. Responsibility for the information and views expressed herein lies entirely with the author(s).

History of the changes

Version	Date	Released by	Comments
1.0	16-03-2018	Sergey Martynov and Haroun Mahgerefteh	First draft

Table of contents

Key word list

Shale gas; Well blowout; Quantitative Risk Assessment

Definitions and acronyms

Acronyms	Definitions
BOP	Blow Out Preventer
CFD	Computational Fluid Dynamics
EoS	Equation of State
QRA	Quantitative Risk Assessment

1. Introduction

1.1 General context

Given the abundant worldwide resources of natural gas trapped in sedimentary shale rock formations ("shale gas"), development of the shale gas resources presents the potential for significantly boosting the countries' economies during the transition from fossil-fuel to more sustainable energy sources[1,2]. However, it is critically important that the design and operation of shale gas facilities meet the required safety standards for minimising or eliminating the risks to the environment and society[1,3].

Work package WP9 is aimed at evaluation of the risks associated with the shale gas extraction[4], in particular focusing on the modelling of the risks of an accidental well blowout and induced seismic/micro seismic activity.

While the induced seismicity caused by hydraulic fracturing has attracted wide public attention, risks associated with the well failure typical of oil and gas operations have received less attention. Review of the past accidents reported for conventional and unconventional gas wells reveals that majority of the few reported well failures and blowouts happened at the exploration stage during drilling into shale formations [5,6].

Due to low porosity of a shale rock, parts of the formation may include gas trapped at very high pressure. Drilling into these areas may result in "pressure kicks", propagating to the wellhead and causing its blowout. To prevent this from happening, safety measures and devises, such as Blow-Out Preventers (BOP), are commonly used in the wells [7]. However, in the unlikely event of the failure of BOP, the resulting pressure kicks may result in uncontrolled release of the gas from the formation, leading to release of the drilling mud and the gas into atmosphere[8], with the subsequent fire and explosion of the gas. Recent examples of shale wells blowouts include, the Acadia Parish well blowout in Louisiana [9] , the Eagle Ford well failure in Texas [10] and most recently the Oklahoma Drilling Accident (https://www.wsj.com/articles/oklahoma-blast-may-be-deadliest-since-start-of-u-s-shale-boom-1516735845). The Acadia Parish well blowout in Louisiana caused fire, explosion and releases of gas and salty water, resulting in evacuation of 40 residents within 1.5 miles from the well and closure of a nearby power plant[9]. Figure 1 shows the fire resulting from blowout of the Eagle Ford shale gas well[10]. Such massive fires can cause significant harm to people in close proximity of the well and the environment, and therefore measures should be taken to minimise the risks of shale gas wells blowouts and mitigate the major accident hazards associated with fires and explosions [11].

Figure 1. A blowout from a well drilled into Eagle Ford shale in Texas [10].

In order to provide the basis for risk mitigation and emergency planning, Quantitative Risk Assessment (QRA) is performed for all major hazards installations. This involves assessment of safe distances to the facility based on modelling of thermal radiation contours from fires and explosion overpressures for relevant failure scenarios. Such methodologies are applied for safety assessment of gas transportation pipelines and storage tanks, and rely on accurate prediction of the transient flowrate and thermodynamic properties of the fluid at the discharge location[12]. In our previous work, we have developed and validated outflow models for simulating accidental releases from high-pressure pipelines transporting various fluids, including hydrocarbons[13,14]. In this deliverable, the pipeline decompression model is adopted to gas wells, and combined with the established fire and explosion models[15,16] to provide the basis for QRA of shale gas wells.

1.2 Deliverable objectives

The present report describes the methodology for evaluation of the consequences of accidental blowout of a shale gas well, and its application to hypothetical scenarios of failure of a realistic shale gas facility.

1.3 Structure of the report

The report is organised as follows. The methodology section describes the models adopted in the present study for prediction of the transient outflow from a shale gas well following a blowout, thermal radiation from the resulting jet fire and the explosion overpressure in the event of a delayed ignition of the released gas.

Next the results obtained using the linked outflow, fire and explosion models based on their application to an hypothetical scenario involving the accidental blowout of a shale gas production well are presented and discussed. The pertinent data required for the modelling are taken from an existing well in the UK for which the relevant design, operational and

prevailing ambient data are available. The simulation model predictions are presented in the form of 2D plots of thermal radiation and explosion over-pressure contours as a function of distance and time following well blowout. This data in turn forms the basis for determining the minimum safety distances taking into account defined thresholds for deferent severity harm scenarios. Conclusions section summarises the main findings and provides a discussion of the practical usefulness of the results in the context of risk assessment of shale wells.

2. Methodology

2.1 Well discharge model

Central to the assessment of the consequences associated with a well blowout is the determination of the ensuing transient discharge rate and the fluid phase composition at the wellhead. In order to predict accurately these properties, a model is constructed accounting for all the important physical processes governing the well blowout process. In particular, to describe the transient flow in a well, a one-dimensional model is adopted, based on the mass, momentum and energy conservation equations [14]:

$$\frac{\partial \rho}{\partial t} + \frac{\partial \rho u}{\partial x} = 0 \qquad (1)$$

$$\frac{\partial \rho u}{\partial t} + \frac{\partial (\rho u^2 + p)}{\partial x} = -\rho g_x - \frac{f_w \rho u^2}{D} \qquad (2)$$

$$\frac{\partial \rho E}{\partial t} + \frac{\partial (\rho u E + u p)}{\partial x} = -\rho u g_x - \frac{f_w \rho u^3}{D} + q_w \qquad (3)$$

where ρ, u, E and p are respectively the fluid density, velocity, total specific energy and pressure, x the spatial coordinate along the well in the direction of discharge flow (from top to bottom), t is the time, and D is the internal diameter of the pipe running along the well. Furthermore, g_x is the local projection of the gravity force on the x axis, q_w is the heat flux at the pipe wall, and f_w is the Fanning friction factor, which in the present study is calculated using Chen's correlation [17]. The model accounts for variation in the inclination of the well with the depth, and can be easily extended to account for the effects of thermal and mechanical non-equilibrium between the fluid phases during the decompression process [14], and variation in the flow area along the well [18].

To enable numerical solution of the above equations, boundary conditions are specified at the top and bottom of the well. In particular, at the bottom location the well is assumed to be connected to an infinitely large reservoir with prescribed formation pressure. Aiming to evaluate hazardous consequences of blowout of a shale gas well for the worst-case scenarios, i.e. upon complete failure the BOP mechanism and full opening of the well to atmosphere at the ground surface, a full-bore rupture boundary condition is used at the top of the well.

Prior to the rupture, the fluid in the well is assumed to be stagnant at temperature equal to the formation temperature with the fluid pressure varying along the well according to the hydrostatic head.

The above governing equations, closed by the set of the initial and boundary conditions along with the physical properties closure correlations, are solved numerically using the finite-volume method [19].

2.2 Jet Fire modelling

In order to predict the flame shape and the subsequent incident thermal radiation following the well blowout, the widely used well-established Chamberlain model [15], [16] for hydrocarbon fires is employed. The model represents the flame as a frustum of a cone (Figure 2), radiating as a solid body with a uniform surface emissive power. In order to determine the geometry of the flame and surface emissive power as functions of the ambient and discharge flow conditions, semi-empirical correlations are used, as described in this section.

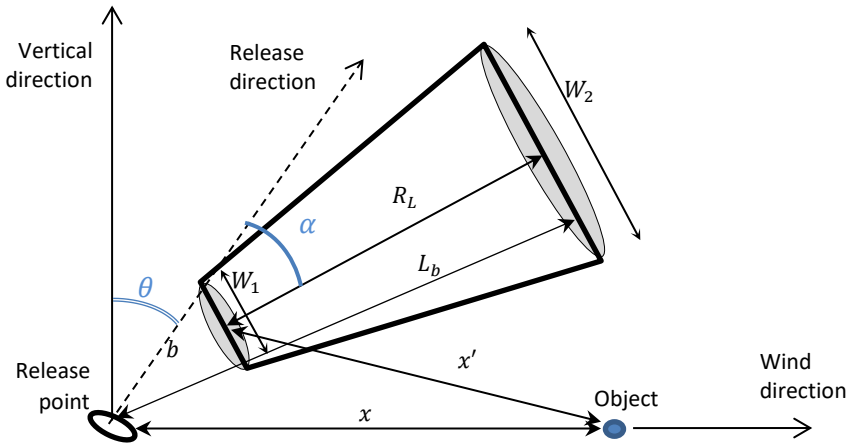

Figure 2. Schematic of the frustum of a cone representing a jet fire in Chamberlain's model [15].

2.2.1 Jet flame geometry

As indicated in Figure 2, the jet flame is characterised by the following set of parameters: b – the lift-off distance between the release point and the frustum base, W_1 and W_2 are the diameters of the frustum base and top faces, respectively, R_L is the visible flame length, L_b is the length of the flame measured from the release point and the tip of the flame. θ is the angle between the release direction and the vertical axis, and α is the tilt angle of the flame.

The above geometric parameters are estimated through a series of semi-empirical correlations [15], dependent on size and orientation of the exit orifice, gas composition and wind speed including its direction and the ambient temperature. The remaining required model source terms obtained from the transient discharge model described above are the release temperature, flowrate, composition and velocity.

2.2.1 Surface emission model

The radiated heat flux by a receiver is determined from:

$$q = \tau \cdot VF \cdot S_\infty \quad (4)$$

where VF is the view factor, describing the geometric relationship between the receiver surface and the flame shape. S_∞ is the average surface emissive power, and τ is the atmospheric transmissivity.

The average surface emissive power of the frustum S_∞ (kW/ m^2) is calculated from:

$$S_\infty = \frac{F_s Q}{A} \quad (5)$$

Where, A is the flame surface area derived from the flame shape (m^2), F_s is the fraction of the combustion energy radiated, and Q is the flame heat intensity (kW). These parameters are determined using the following models.

The frustum surface area, A (m^2) is calculated knowing the diameters of the frustum at its base and the top (Figure 2):

$$A = \frac{\pi}{4}\left({W_1}^2 + {W_2}^2\right) + \frac{\pi}{2}(W_1 + W_2)\sqrt{{R_L}^2 + \left(\frac{W_2 - W_1}{2}\right)^2} \quad (6)$$

Assuming adiabatic expansion and complete combustion, the radiated power, Q, is defined as:

$$Q = \dot{m}\Delta H_c \quad (7)$$

Where, ΔH_c (kJ/kg) is the standard enthalpy of combustion of the gas, and $\dot{m}$ is the gas discharge mass flow rate (kg/s).

For large flames, F_s is approximately correlated with the gas jet velocity, u_j [15]:

$$F_s = 0.21e^{-0.00323u_j} + 0.11 \quad (8)$$

Assuming the flame black body radiation temperature of 1500 K, and the atmospheric transmissivity is due to absorption and re-radiation by CO_2 and H_2O(g), the atmospheric transmissivity is approximated as [20]:

$$\tau = 1.006 - 0.01171log_{10}X(H_2O) - 0.02368\left(log_{10}X(H_2O)\right)^2 - 0.03188log_{10}X(CO_2) + 0.001164\left(log_{10}X(CO_2)\right)^2 \quad (9)$$

where $X(H_2O) = R_H P_L S_{mm}(288.65/T_{air})$, $X(CO_2) = P_L(273/T_{air})$, R_H is the relative humidity, P_L is the path length (m), T_{air} is the ambient temperature (K) and S_{mm} is the saturated water vapour pressure in mmHg at the ambient temperature.

2.2.2 Safe distance calculations

The previous section described the methodology for the calculation of the spatial variation of the thermal radiation heat flux, q with the distance to the flame as a function of time following the well blowout. This information can in turn be used to determine the minimum safe distances corresponding to the various defined thresholds for different degrees of harm to people and steel structures[21].

2.2 Explosion modelling

In practice, the accidental blowout of shale gas wells will result in the escape of gas into a space partially obstructed by equipment and constructions near the well pad during the drilling and fracturing operations. The delayed ignition of the release gas will lead to an explosion, creating a blast wave propagating away from the release point. The resulting explosion overpressure associated with the blast wave may pose a significant safety hazard to people and surrounding structures and should therefore be quantified as a part of the safety assessment. For this purpose, the widely established and validated TNO Multi-Energy Vapour Cloud Explosion Model[16] is employed in the present study. Linked to the transient well discharge model (section 2.1) as the source term, the model predicts the blast overpressure at various distances away from the release point at different time intervals for both un-obstructed and partially obstructed surroundings.

The peak overpressure, P_s created by the blast wave at the ground level is determined using empirical lookup tables provided in the TNO report[16] as a function of explosion blast strength, $P_s' = P_s/P_a$, (here P_a is the atmospheric pressure) and the dimensionless radial distance to the explosion source, $r' = r\ \sqrt[3]{p_a/E}$, (here r and E are respectively the radial distance from the ignition source and the blast energy)

Conservatively, based on realistic tests, for unconfined vapour cloud explosions, the blast strength, P_s', is set to 3. In cases of partial or full confinement, the blast wave is assumed to run only in obstructed regions[16], where P_s' can be set to 10.

Furthermore, the blast source containing a combustible fuel-air mixture is modelled as a hemi-sphere of radius, r_o(m):

$$r_o = \frac{3E}{2(E_v \times \pi)^{1/3}} \quad (10)$$

where E_v (J/m^3) is the heat of combustion of the stoichiometric hydrocarbon-air mixture per unit volume[16], and E (J) is the energy of the blast wave defined as:

$$E = E_v V \tag{11}$$

where V(m^3) is the volume of the cloud in specific region of interest. For fully or partially confined explosions, V is set to the volume of confinement, V_{gr} (m^3). For unconfined explosions on the other hand, V corresponds to the volume of fully expanded cloud:

$$V = V_c - V_{gr} \tag{12}$$

where V_c (m^3)is the volume of the released combustible gas cloud, which is calculated as:

$$V_c = \frac{Q_{ex}}{\rho\, \alpha_s} \tag{13}$$

where ρ (kg/m^3) is the cloud density, α_s is the air-fuel stoichiometric concentration (vol%). Q_{ex} (kg) is the amount of vapour released, as predicted using the well discharge model presented in section 2.1.

2.3 Physical properties

Natural gas from shale formations is composed of mainly methane (usually >80%)[22,23] mixed with additional components, which vary in the nature and amount depending on the type of formation. In most cases, these primarily include ethane, propane, and butane along with heavier alkanes and non-combustibles such as N_2, CO_2 and H_2S. Given uncertainty of the shale gas composition, the present study is performed for pure methane representing the worst case scenario.

To obtain the physical properties of natural gas, PC-SAFT[25] and Peng-Robinson (PR)[26] Equations of State (EoS) can be used. While PC-SAFT is claimed to produce accurate description of the properties, including the vapour-liquid phase equilibrium data, our investigations revealed that for the range of typical natural gas compositions (including pure methane), temperatures and pressures (Figure 5) likely to be encountered in practice, the Peng-Robinson equation provided close agreement. Given the significantly lower computational run time afforded by the PR EoS once implemented in the well discharge model as opposed to PC-SAFT, the former EoS was employed in the following investigations.

3. Results and discussion

3.1 The case study

The hypothetical blowout of the shale gas well constructed by Cuadrilla Elswick Ltd in Roseacre Wood, Lancashire, UK[27] leading to a fire or an explosion is used as a case study involving the application of the transient blowout model developed in this work. The well geometry, the site layout and meteorological data, as well as characteristics of the shale formation at various depths is documented in several reports[27–29]. The relevant data required for conducting the case study failure simulation is presented in the following.

Figure 3 shows schematically the dimensioned vertical and horizontal sections of four wells drilled into the formation. All four wells are target the Bowland Shale and Hodder Mudstone formations at the depths between 1500 m and 3000 m. All the wells, apart from a branch of well 1, include 1000-2000 m long horizontal sections. Given that no details are available about the actual inclination profile of the wells, the present study is performed for a vertical well with the production liner of a nominal diameter of 114.3 mm and length of 4000 m.

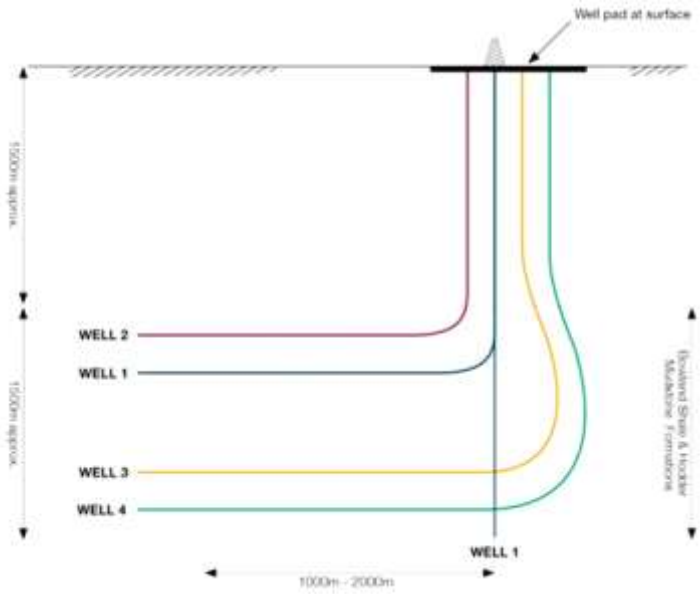

Figure 3. Schematics of the shale gas exploration wells in the Roseacre Wood project [29].

The gas pressure and temperature at the bottom of the well are prescribed based on the data reported for the Lower Bowland shale formation; Figure 4. In particular, the shale gas temperature is set to 343 K, while the gas pressure is varied between 200 and 600 bar; the latter covering the range between hydrostatic and lithostatic pressures in the shale formation. The lithostatic pressure gives an estimate of the maximum pressure that could be encountered when drilling into the formation, e.g. resulting in a “gas kick”, potentially leading to the well failure [30].

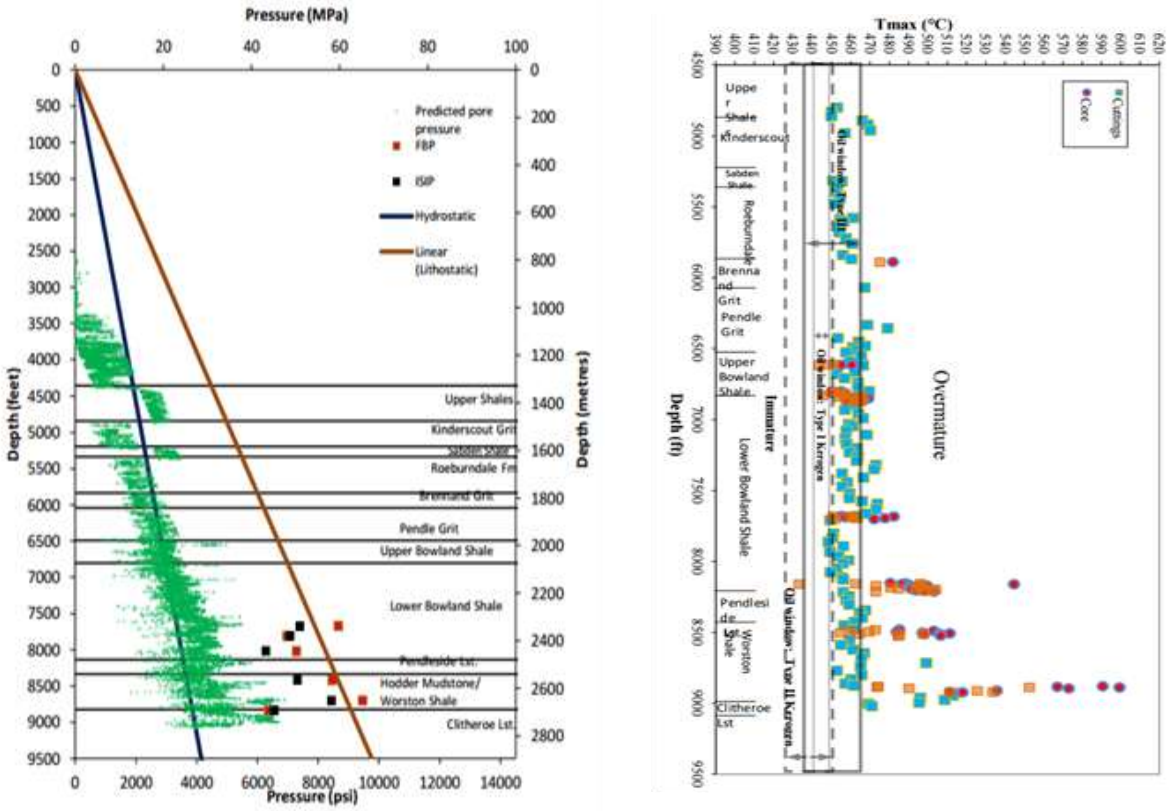

Figure 4. Variation of pressure (a) and temperature (b) with depth at the Rose Acre Wood site [28].

In order to evaluate the hazard consequences for *a worst case scenario* of well blowout, the unlikely full-bore rupture of the well is simulated.

The surrounding air is assumed to be at 20°C, and 50% humidity. Based on the meteorological data[29], the wind speed at the ground surface on the site is taken as the maximum value of 10 m/s. Furthermore, the release is assumed to be vertical, while the heat exchange between the well and the formation is neglected. The main parameters for the well blowout simulation case study are listed in Table 1.

Table 1. Main characteristics of the well and the reservoir conditions for blowout simulation

Parameters	Value
Well parameters	
Overall length	4000 m
Material of construction	Mild steel
Wall surface roughness	0.05 mm
Heat transfer coefficient	0 W/m^{2}K (Adiabatic)
External diameter	127 mm
Internal diameter	114.4 mm
Wall thickness	6.2 mm
Orientation relative to horizontal	90 ^{o} (vertical)
Reservoir parameters	
Temperature	343 K
Pressure	200 bar

Application of the gas explosion model described in section 2.3 requires specification of the local level of confinement. Figure 5 shows the Rose Acre Wood site layout with four wells and drilling activities at one of the wells. Figure 6 gives is photograph as an example of on-site installations at the drilling phase of shale gas exploration. The minimum area occupied by equipment (e.g. drilling pumps) on the site near the well can be estimated to be *ca* 10 m^2, while the total area of the sites is *ca* 100 x 130 m^2. As such, for the purpose of the present study, the volume of confinement, V_{gr}, is varied in the range from 10 to 10^4 m^3.

It should be noted that to protect the site during the drilling activities, provision is made for two protection fences of 2.4 m and 4 m in height, and separated by distance *ca* 6.5 m, surrounding the site area (Figure 5 and Figure 7). From Figure 7 the distance between the fences and the wells can be estimated to be ca 30 m, while in Figure 5 the distance from the well to the buildings within the site area varies between *ca* 40 and 80 m. While the consequence modelling in the present study assumes no physical protection barriers around the well, the study will provide independent evaluation of the safe distances, as the key inputs for the design of emergency mitigation measures such as blast walls.

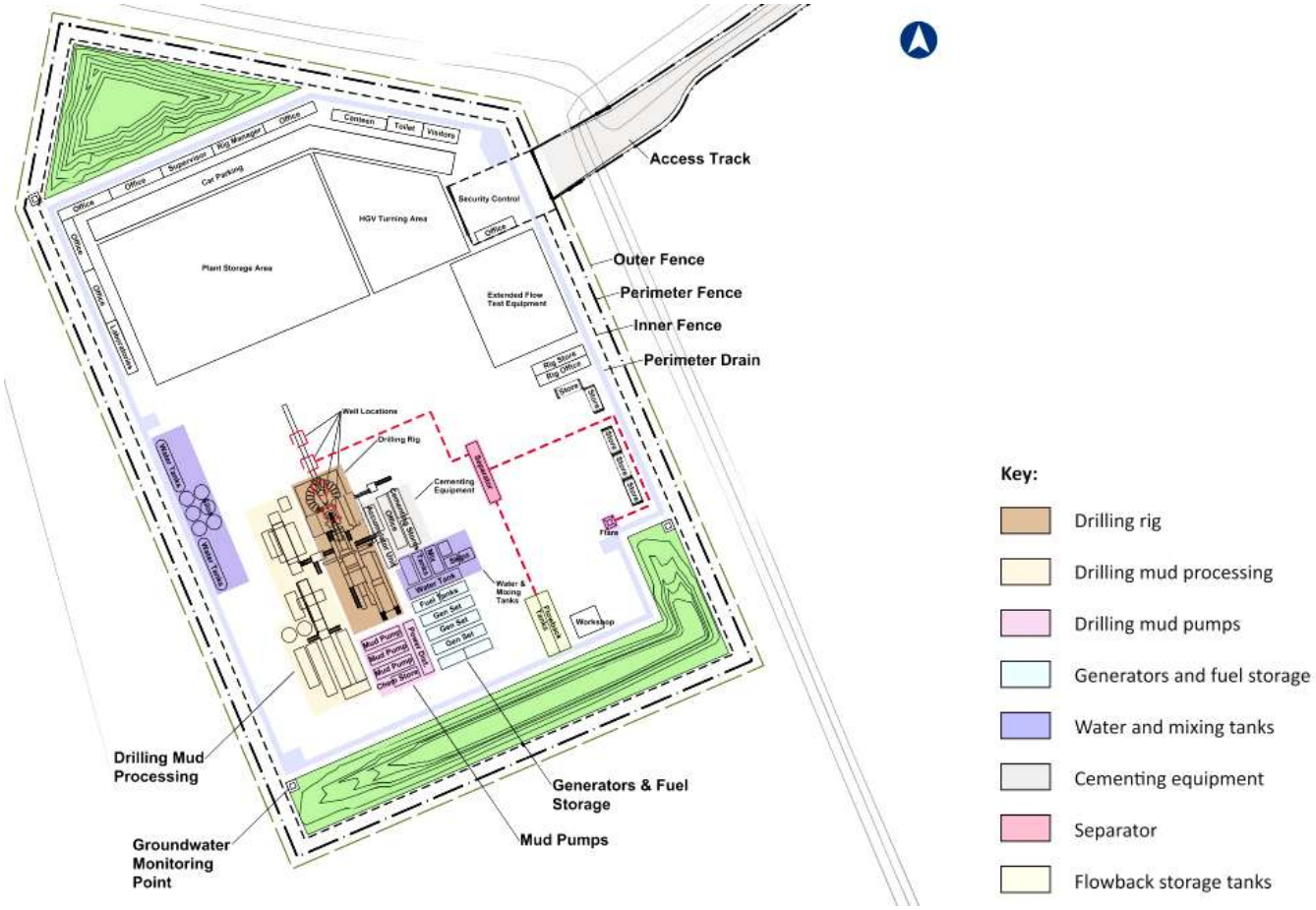

Figure 5. The layout of the Roseacre Wood well pad site for the shale gas exploration drilling and testing activities with the drilling rig surrounding one well, showing the various equipment and safeguarding fences around the site[31]. The site area is ca 100 m x 130 m.

Figure 6. Photograph of the Cuadrilla shale gas drilling rig in Preese Hall [32]

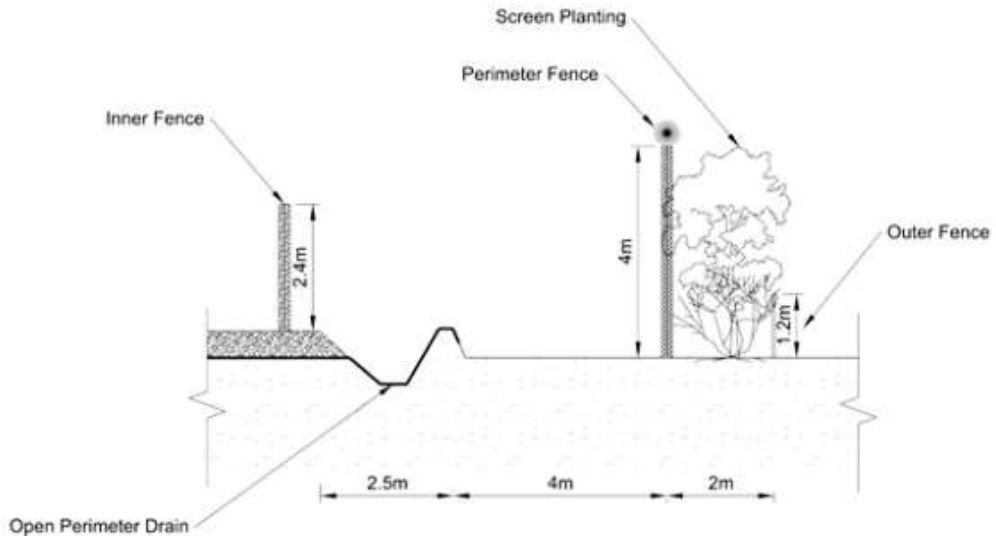

Figure 7. Example of safety and security barriers designed for the Rose Acre Wood shale gas exploration project [27].

3.2 Jet fire simulation

In this section the results of calculations of thermal radiation and safe distances from jet fires formed following accidental blowout of the shale well (Table 1) are presented and discussed. The results are obtained for vertical flames in open space with no thermal barriers. The failure simulations cover the well pressures of 200, 400 and 600 bar and the wind speeds of 0 and 10 m/s.

Figure 8 shows the instantaneous incident heat flux radiation contours at the ground level within +/- 200 m from the jet flame at 0.5, 2, 10 and 50 s after the well blowout. The results correspond to zero wind speed and 200 bar formation pressure. It can be clearly seen that the incident heat flux decreases with the distance from the centre of the jet and also decays with the time, reaching its maximum of *ca* 3 kW/m^2 at *ca* 20 m distance from the well at time interval of 30 s.

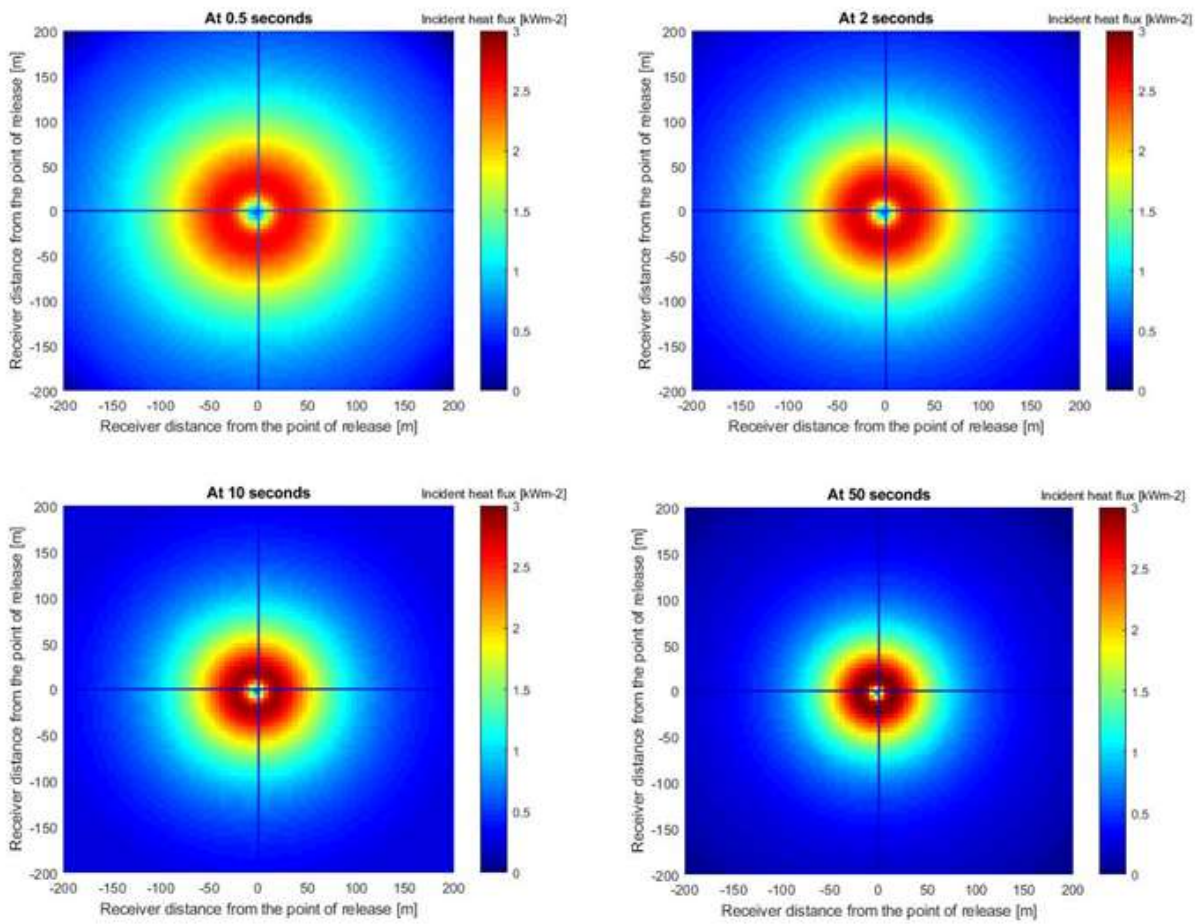

Figure 8. Incident heat flux contours at the ground level around vertical flame formed from the wellhead at (0;0), predicted at 0.5, 2, 10 and 50 s following blowout. Wind speed = 0 m/s.

Figure 9 shows the variation of the instantaneous incident heat flux as a function of distance from the flame source at different time intervals of 10s and 50s under calm weather (no wind) and 10 m/s wind speed conditions. While the data in the plots shows a small variation of heat flux with the time, the thermal radiation is a strong function of both the receiver distance and the wind speed.

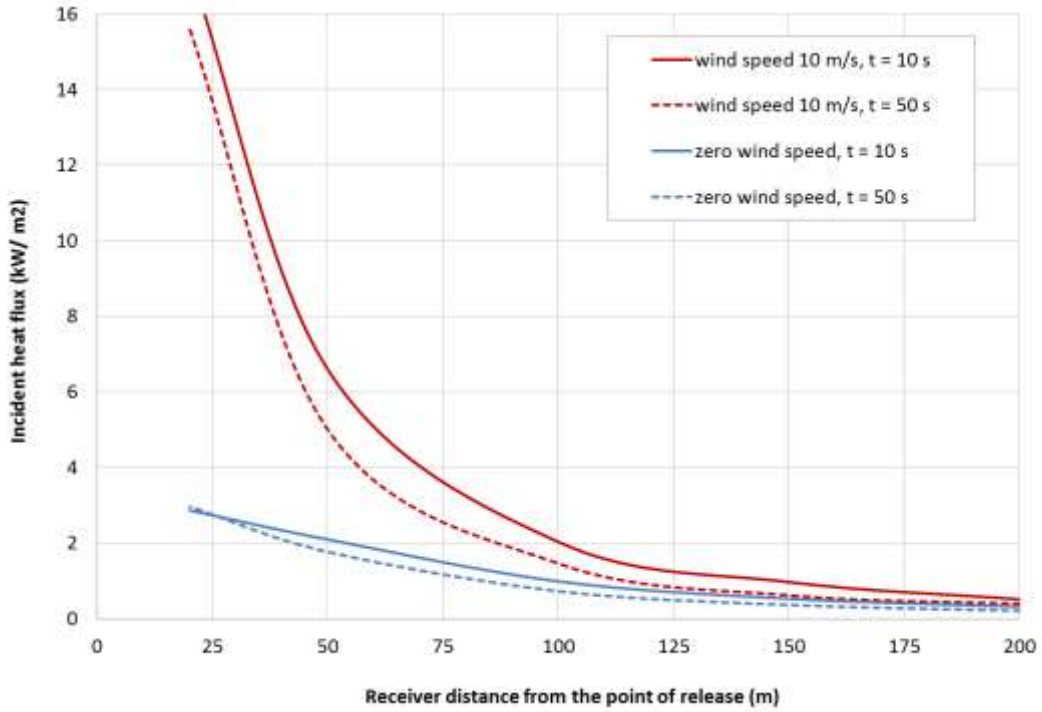

Figure 9. The incident radiation heat flux as a function of the receiver distance, predicted at 10 and 50 s during the vertical well blowout for zero and 10 m/s wind speeds.

The severity of the thermal radiation hazard (the thermal radiation dose) depends on the radiation intensity at a specific location and the receiver exposure time.

Error! Reference source not found. presents the durations of exposure to various levels of heat radiation flux that may cause severe pain and the second degree burn for bare skin.

Table 2. Time for physiological effects on bare skin following exposure to various heat radiation flux levels as a result of a fire [33].

Thermal radiation flux (kW/m^2)	Exposure time leading to severe pain (s)	Exposure time leading to 2nd degree burn (s)
1	115	663
2	45	187
3	27	92
4	18	57
5	13	40
6	11	30
8	7	20
10	5	14
12	4	11

The results in Figure 9 followed by reference to Table 2, may be used to determine the minimum safe distances where exposure to the well blowout fire for a various durations may pose serious harm to people.

The based on Figure 9, a heat radiation flux of 2 kW/m^2 is predicted at *ca* 50 m and 100 m from the well for zero and 10 m/s wind speeds respectively. Based on the data in **Error! Reference source not found.**, exposure to this level of radiation for a period of 40 s may result in severe pain, while exposure exceeding 187 s may cause second degree burn.

Based on the results of the calculations of the thermal radiation from the jet flame, those locations where the incident heat flux drops below a certain hazardous threshold level, can be determined. In particular, *minimum safe distances* to personnel and steel structures where the incident heat flux reaches 3.5 and 36 kW/m^2, respectively[21] may be determined.

Figure 10 shows the simulated variations of the minimum safe distances to personnel (6.3 kW/m^2 threshold) and steel structures (35 kW/m^2 threshold) for jet fires formed following well blowout for formation pressures of 200, 400 and 600 bar. A wind speed of 10 m/s is assumed.

As it may be observed, at all the times the safe distances to the personnel are nearly 2 to 2.5 times larger than those required for the steel structures. Also, at any given formation pressure, the minimum safe distance initially rapidly increases with time upon blowout, consistent with the massive release. This trend is next followed by a much less marked reduction in the minimum safe distance as the well gradually depressurises.

Longest safe distances in Figure 10 are predicted at the moment of release where the discharge rate and the flame length are at their peak values. Based on this worst case scenario, the minimum estimated safe distance for personnel is *ca* 140 m, while that for steel structures is 40 m away from the well. The latter finding is consistent with the plant layout shown in Figure 5 where offices, workshop and store houses are placed at *ca* 50 m from the wells.

The results also show that the safe distance increased only slightly (by less than 1%), when the presence of impurities is the natural gas is taken into account (C_2H_6 - 4.5mol%, C_3H_8 - 3.5mol%; C_4H_{10} - 2mol%).

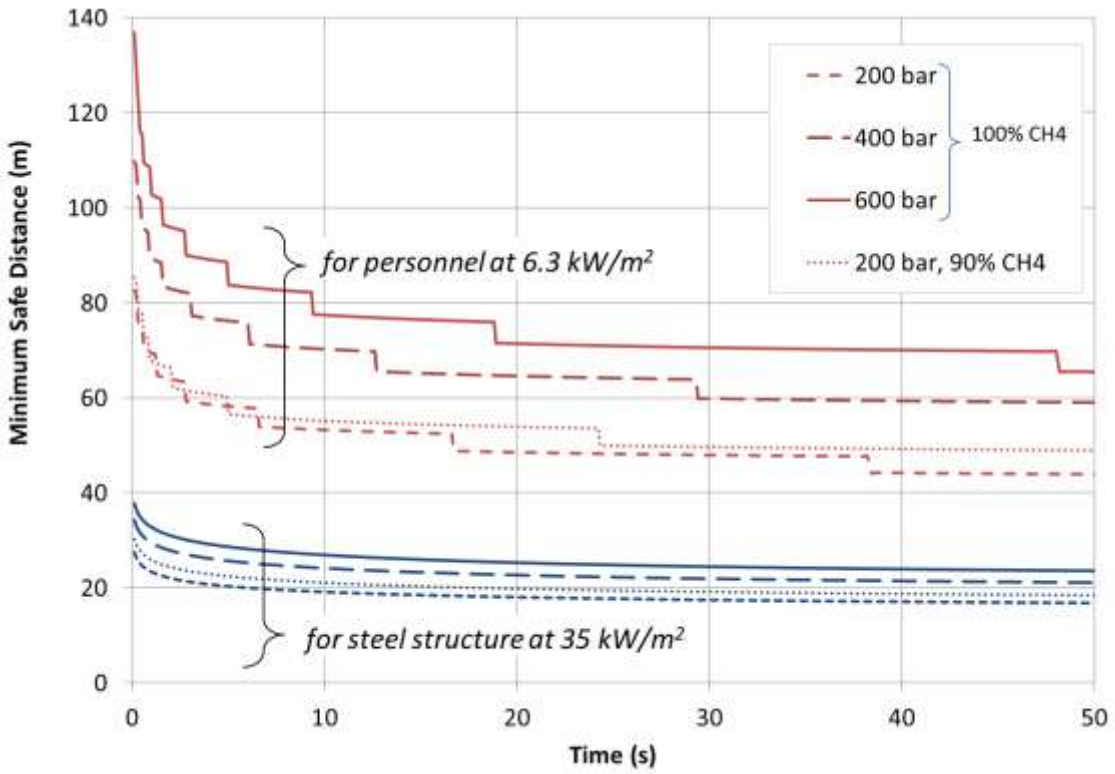

Figure 10. Safe distances to a vertical flame for personnel (outside the buildings and unprotected) and steel structures, calculated for 200, 400 and 600 bar formation pressures for the baseline scenario (pure methane) and natural gas containing 90 mol% of methane (C_2H_6 - 4.5 mol%, C_3H_8 - 3.5 mol%; C_4H_{10} – 2 mol%). Wind speed 10 m/s. The terrain is assumed to be flat with no firewalls in place.

3.3 Explosions

In the following, the results of simulations of blast overpressures are presented and discussed in the context of safe distances for personnel working at the well site. Given that the site equipment and facilities represent partial obstruction to the explosion, to account for these, the volume of confinement, V_{gr}, is varied between 10 and 10,000 m^3. These are representative, of one-storey buildings (3 m high) with the length and width ranging from *ca* 2 to 55 m.

For the sake of example, the results are obtained for 200 bar formation pressure. Following the TNO recommendations, the blast strengths are respectively set to 3 bar and 10 bar for explosions in unconfined and partially spaces [16]. An arbitrarily ignition delay of 1 s following a well blowout is assumed.

Figure 11 shows the simulated variation of the peak overpressure as a function of distance from the explosion source located at the well head following well blowout. The results are plotted for various volumes of confinement, V_{gr}. The two hazardous overpressure

thresholds of 70 mbar 300 mbar relevant to personnel working in open space areas and in buildings are also indicated in the same figure.

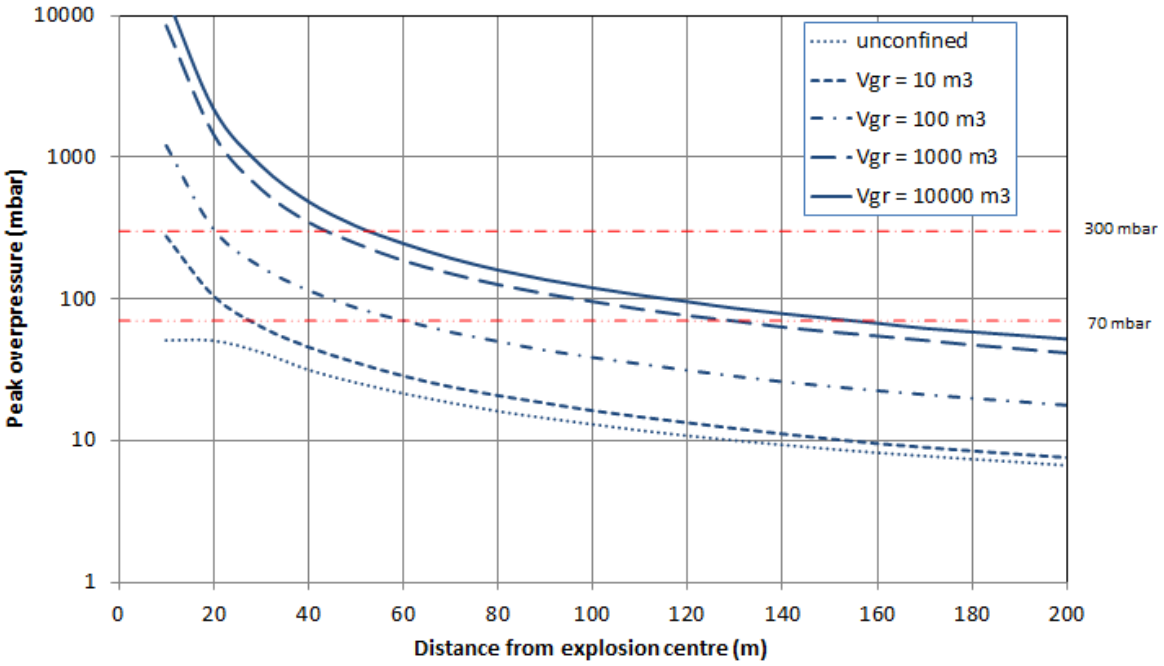

Figure 11. Explosion overpressure predicted as a function of distance from the explosion source for various levels of confinement.

The results of the explosion over-peak pressure calculations for the natural gas composed by 90% of methane mixed with 4.5mol% of C_2H_6, 3.5mol% of C_3H_8 and 2mol% C_4H_{10} showed no practically noticeable difference with the results presented in Figure 12 for the baseline case of pure methane.

Table 3. Potential damage and fatalities peak overpressure thresholds for people working in different types of buildings [33].

Type of location	Peak overpressure (mbar)	Potential damage
People in the open	300	Eardrum rupture
	1000	Picked up and thrown; likely fatality
People in normal buildings	70 - 250	Significant likelihood of fatality due to masonry collapse and projectiles, particularly glass
Blast resistant buildings	> 200	Some likely fatality
Blast proof buildings	> 1000	Some likely fatality

Error! Reference source not found. shows peak overpressures corresponding to various types of injuries for people working in different types of locations in the event of a vapour cloud explosion. According to the data in Table 3, for people in open spaces, the blast overpressures above 300 mbar can cause significant injuries such as eardrum rupture. The results in Figure 12 show that explosion overpressures above 300 mbar can be expected to be within ca 10 m to 50 m radius from the explosion centre for the confinement volumes between 10 and 10,000 m^3 respectively.

For people inside normal buildings, Table 3 suggests 70 mbar as potentially fatal overpressure threshold. From Figure 12 it can be seen that overpressures above 70 mbar can be expected within ca 150 m radius from the explosion centre for highly-obstructed regions (V_{gr} = 10,000 m^3) and less than 60 m for low-obstructed regions (V_{gr} = 100 m^3).

As such, the simulated overpressure data indicate no risk of fatalities for people in normal buildings located at more than 60 m away from an explosion originating at the drilling pad . In this case, the maximum predicted explosion overpressure falls below the 70 mbar threshold needed to cause a fatality. This finding is consistent with the plant layout shown in Figure 6, where offices, stores, workshop and laboratories (apart from the cementing unit office) are placed at more than 50 m away from the wells.

4. Conclusions and future steps

This deliverable described the development and application of a methodology for determining the minimum safe distances to personnel and equipment in the unlikely event of a blowout of shale gas wells.

This task involved the integration of a transient CFD outflow model, serving as the source term, with established empirically based correlations for predicting the subsequent jet fire incident heat flux, and in the event of a delayed ignition following the well blowout, the resulting explosion over-pressures for both unconfined and partially confined surroundings.

The model's testing is based on its application to hypothetical scenarios involving well blowout at the Rose Acre shale gas exploration site in the UK. Worst case scenario corresponding to a blowout during the drilling stage is assumed. The simulation results are presented in the form of 2D plots of thermal radiation contours as a function of distance and time and explosion over-pressure/distance profiles for an arbitrary 1 s delay in the detonation of the released gas.

Parametric studies are conducted in order to demonstrate the impact of changes in the formation pressure and wind speed on the resulting jet fire incident heat flux and explosion over-pressure, the latter for different degrees of confinement.

The minimum distances coinciding with various degrees of harm including 2nd degree burns, explosion injuries or fatalities are determined by reference to the relevant published fire and explosion harm thresholds.

The well blowout simulation study indicates that fire and explosion hazard consequences are minimal for personnel working in buildings located at distances of more than 60 m away from the wellheads. These findings are qualitatively consistent with layout of the Rose Acre Wood shale gas site where the buildings are sited over 60 m away from the wellhead.

In conclusion, the modelling and the methodology presented in this report is shown to serve as a useful tool for quantitative risk assessment of shale gas facilities, to ensure safe design layout and thereby minimising the consequences of a well blowout.

References

(1) The Royal Society. *Shale Gas Extraction in the UK : A Review of Hydraulic Fracturing*; London, 2012.

(2) Melikoglu, M. Shale Gas: Analysis of Its Role in the Global Energy Market. *Renew. Sustain. Energy Rev.* **2014**, *37*, 460–468.

(3) HSE. *Shale Gas and Hydraulic Fracturing (Fracking) Q & A*; 2012.

(4) ShaleXenvironmenT. *Maximizing the EU Shale Gas Potential by Minimizing Its Environmental Footprint. H2020 Proposal. Description of Work.*; 2015.

(5) Willson, S. A Wellbore Stability Approach For Self-Killing Blowout Assessment. *SPE Deep. Drill. Complet. Conf.* **2012**, No. June, 20–21.

(6) Duncan, I. Likelihood and Environmental Consequences of Blowouts of Shale Gas and Shale Oil Wells. **2016**, 9–11.

(7) Skalle, P. *Pressure Control During Oil Well Drilling*, 6th ed.; bookboon, 2015.

(8) Boak, J. *Chapter 6. Shale-Hosted Hydrocarbons and Hydraulic Fracturing*; Elsevier Ltd, 2014.

(9) KLFY.com. No injuries in well blowout in Acadia Parish http://klfy.com/2014/02/26/no-injuries-in-well-blowout-in-acadia-parish/.

(10) Dukes, R. T. Eagle Ford Well Blowout Near Petersville - EOG & Nabors https://eaglefordshale.com/efs-news/news/eagle-ford-well-blowout-near-petersville-eog-nabors.

(11) Department of Energy and Climate Change. Onshore Oil and Gas Exploration in the UK: Regulation and Best Practice. *https://www.gov.uk/government/uploads/system/uploads/attachment_data/file/265988/Onshore_UK_oil_and_gas_exploration_England_Dec13_contents.pdf* **2015**, No. December.

(12) Mahgerefteh, H.; Oke, A. O.; Rykov, Y. Efficient Numerical Solution for Highly Transient Flows. *Chem. Eng. Sci.* **2006**, *61* (15), 5049–5056.

(13) Mahgerefteh, H.; Saha, P.; Economou, I. G. Fast Numerical Simulation for Full Bore Rupture of Pressurized Pipelines. *Aiche J.* **1999**, *45* (6), 1191–1201.

(14) Brown, S.; Martynov, S.; Mahgerefteh, H.; Proust, C. A Homogeneous Relaxation Flow Model for the Full Bore Rupture of Dense Phase CO2 Pipelines. *Int. J. Greenh. Gas Control* **2013**, *17*, 349–356.

(15) Chamberlain, G. A. Developments in Design Methods for Predicting Thermal Radiation From Flares. *Chem. Eng. Res. Des.* **1987**, *65* (July 1987), 299–309.

(16) TNO. *Methods for the Calculation of Physical Effects*, 3rd Editio.; van den Bosch, C. J. H., Weterings, R. A. P. M., Eds.; TNO: The Hague, 2005.

(17) Chen, N. H. An Explicit Equation for Friction Factor in Pipe. *Ind. Eng. Chem. Fundam.* **1979**, *18* (3), 296–297.

(18) Brown, S.; Martynov, S.; Mahgerefeth, H. Simulation of Two-Phase Flow through

Ducts with Discontinuous Cross-Section. *Comput. Fluids* **2015**.

(19) Toro, E. F. The HLL and HLLC Riemann Solvers. In *Riemann Solvers and Numerical Methods for Fluid Dynamics*; 1997; pp 293–311.

(20) Phillips, L. *Shell FRED Technical Guide*; Shell Research Ltd.: Chester, England, 2007.

(21) Lees, F. P. *Lees' Loss Prevention in the Process Industries: Hazard Identification, Assessment and Control*, 3rd ed.; Mannan, S., Ed.; Elsevier, 2005.

(22) Stamford, L.; Azapagic, A. Life Cycle Environmental Impacts of UK Shale Gas. *Appl. Energy* **2014**, *134*, 506–518.

(23) Whitelaw, P.; Uguna, C.; Stevens, L.; Meredith, W.; Snape, C. E.; Vane, C.; Carr, A. D. An Evaluation of Shale Gas Potential in the Bowland Shale , UK Using Sequential High Water Pressure Pyrolysis and Methane Adsorption *. **2017**, *51450*.

(24) MacKay, D. J.; Stone, T. J. Potential Greenhouse Gas Emissions Associated with Shale Gas Extraction and Use. *UK Dept Energy Clim. Chang.* **2013**, No. September, 1–50.

(25) Behaviour, P.; Boulougouris, G.; Tsangaris, D. M.; Economou, I. G. PC-SAFT + Electrolyte (ePC-SAFT) EoS Developed and Validated for at Least 3 CO 2 Mixtures. **2014**, No. 309102, 1–19.

(26) Wu, D.; Chen, S. A Modified Peng-Robinson Equation of State. *Chem. Eng. Commun.* **1997**, *156* (1), 215–225.

(27) Cuadrilla Elswick Ltd. Exploration Works Planning Application. **2014**, No. June.

(28) Turner, P. *UK Shale Gas Exploration, Cuadrilla Resources Ltd*.

(29) Cuadrilla Elswick Ltd. *Environmental Statement*; 2014.

(30) Groat, C. G.; Grimshaw, T. W. Fact-Based Regulation for Environmental Protection in Shale Gas Development Fact-Based Regulation for Environmental Protection in Shale Gas Development. Summary of Findings. **2012**, 59.

(31) Egan, F. *Emerging Findings of the Environmental Impact Assessment: Roseacre Wood*; 2014.

(32) Cuadrilla Resources. UK : Cuadrilla Resources Releases Report on Unusual Seismic Activity Related to Lancashire Shale Gas Drilling. *Energy-pedia News* **2011**, No. Nov 2011, 1–5.

(33) DOT. *Handbook of Chemical Hazard Analysis Procedures. Federal Emergency Management Agency, U.S. Department of Transportation, and U.S. Environmental Protection Agency.*; Federal Emergency Management Agency Publications Office: Washington, D.C., 1988.